MIXED MODE FRACTURE ASSESSMENT FOR BOX GIRDER WITH CRACK DAMAGE UNDER COMBINED LOADS

(Reference NO. IJME713, DOI No. 10.5750/ijme.v163iA4.26)

Z Y Peng, and **P Yang,** Key Laboratory of High-Performance Ship Technology (Wuhan University of Technology), and School of Naval Architecture, Ocean and Energy Power Engineering, Wuhan University of Technology, China; **Y L Song** and **K Hu,** School of Naval Architecture, Ocean and Energy Power Engineering, Wuhan University of Technology, China

KEY DATES: Submitted: 07/04/21; Final acceptance: 27/01/22; Published 07/04/22

SUMMARY

The box girder is an important structure widely used in the ship and marine engineering, but the fracture problem is not extensively investigated. The paper adopts the stress intensity factor (SIF) as the fracture parameter to perform the three-dimensional (3D) mixed mode fracture assessment of the box girder structure with crack damage. The bending load, torsion load and side load are first introduced to study box girder fracture behavior. And the related influencing factors including crack lengths, crack angles and combined loads are investigated emphatically. Besides, the crack growth angle is also investigated to evaluate the crack propagation behavior. The results show that the load types have a significant effect on the crack propagation. The effect of bending load is generally greater than torsion load. The combined effect of bending and torsion loads may be considered adopting a linear superposition principle under transverse crack and larger angle crack. Additionally, the SIFs produced by torsion load only have a slight change with the increased crack angles. When the side load is added, the area near the crack upper surface will be easy to occur unstable expansion. These findings from the present study will provide a guiding significance to evaluate the crack propagation of box girder under combined loads.

NOMENCLATURE

a	Width of box girder (mm)
b	Length of box girder (mm)
c	Crack length (mm)
$2c$ / a	Dimensionless crack length
E	Elastic modulus (GPa)
h	Depth of box girder (mm)
h_0	Transverse frame height (mm)
K_{I}	Mode-I SIF (MPa·mm$^{1/2}$)
K_{II}	Mode-II SIF (MPa·mm$^{1/2}$)
K_{III}	Mode-III SIF (MPa·mm$^{1/2}$)
K_{eff}	Effective SIF (ESIF) (MPa·mm$^{1/2}$)
SIF	Stress intensity factor (MPa·mm$^{1/2}$)
t	Plate thickness (mm)
t_0	Transverse frame thickness (mm)
θ	Crack angle (°)
θ_0	Crack growth angle (°)
v	Poisson′s ratio

1. INTRODUCTION

The box-shaped thin-walled structure has great strength and stiffness and is widely used in large-scale structural engineering fields such as aerospace engineering, ship and ocean engineering, bridge engineering, cranes, etc. And the incidence of flaws such as cracks is inevitable in their lifetime. When the box girder is subjected to external loads (such as bending, torsion loads and side load), its fracture performance has gradually become a concerned problem. However, the current literatures on the box girder mainly focus on the evaluation of bearing capacity. Shi & Wang (2012) investigated the residual ultimate strength of box girder with crack damage under torsion loading, but they did not further study fatigue fracture of structure. Cui & Yang (2018) investigated the failure characteristics of two box girder models under the cyclic bending moment. The results indicate that every bending moment may cause the larger deformation, which will reduce the fatigue strength and ultimate bearing capacity of box girder. As can be seen, the studies about the fracture issues of box girder are still rarely involved due to the special structural features.

For structural fracture problems, the evaluation methods based on fracture mechanics have been widely used in various engineering fields (Li, 2007). Stress intensity factor (SIF) is used to consider as an important fracture parameter for assessing the fracture failure of structures, which has been effectively verified in many studies. At present, the methods of evaluating stress intensity mainly include displacement extrapolation method (Xuan *et al*., 2006; Awang *et al*., 2018), interaction integration method (Chen *et al*., 2018; Hou *et al*., 2018), extended finite element method (Pang *et al*., 2016; Benvenuti, 2017; Peng & Yang, 2020), etc. These methods play a major role in predicting stress intensity factors accurately. For more engineering mechanics problems, there is a significant problem in fracture mechanics involving “true” three-dimensional nature (Ayhan & Demir, 2019). So, the two-dimensional ideal hypothesis analysis may be insufficient to meet the actual need. Recently, the three-dimensional fracture problems have been investigated a lot by many scholars. Xu *et al*. (2016) carried out the experiment and finite element analysis on 300Mn steel MT test specimens for aircraft landing gear. The results indicate that the thickness has a certain effect on the mode-I SIFs. Huang *et al*. (2017) studied the effect of load modes and out-of-plane bending on stiffened plate fracture by means of

evaluating 3D SIFs. They found that the load modes and out-of-plane bending might affect the distribution law of K_I along the crack front, which had a significant effect on crack propagation. Xiong *et al*. (2016) established the crack sub-model of crane box girder based on the shell-solid sub-model technology, and deeply discussed the influence of crack size and structural parameters on the fracture parameters. Li *et al*. (2020) proposed a simple and practical equation to predict the SIFs (K_I) of thin-walled box girder with cross-shaped crack and periodic T-shaped crack in bending load condition. The research objects are mainly MT specimens, CT specimens, flat plates, stiffened plates and other simple basic structures, but not many large and complex structures are touched. Moreover, these studies are mainly about a single fracture mode, and the variation laws of SIFs along the thickness direction are also rarely touched in multiple modes conditions.

In actual, engineering structures are mostly composite fractures rather than single fracture mode. There are three types of fracture modes, namely mode-I, mode-II, and mode-III (Anderson, 2005). Mode-I means that the applied load is normal to the crack plane and the crack is in an open state. Mode-II refers to the in-plane shear mode, which tends to make one crack surface slide relative to the other. Mode-III corresponds to out-of-plane shear. The mixed mode can be any two or a combination of the three above modes. Numerous scholars have conducted a series of scientific studies on various aspects about mixed mode fractures. Irfaee & Mahmound (2019) conducted the mixed-mode fracture research for steel twin box girder bridge. They proposed a systematic method to evaluate the fracture-critical bridge using the important fatigue fracture parameter (SIFs), but there is no further study on the influence of bending and torsion loads. Compared with the box girder structure, the basic structure has achieved remarkable results in experiments and numerical simulations. In experimental investigations, Seifi & Omidvar (2013) studied the mixed mode I/III by improved CT specimen. With the increase of initial angle and crack length, K_I decreases while K_{III} increases, and the effect of K_{II} is negligible for this specimen. Demir *et al*. (2019) adopted a new experimental test system to further investigate the mixed mode-I/II/III fracture. And they proposed a new improved mixed fracture criterion. In numerical investigations, Li *et al*. (2011) carried out a three-dimensional inclined crack analysis on MCTS specimens, and analyzed the variation law of three different modes of SIF in the thickness direction, namely K_I, K_{II}, and K_{III}. The results show that the area near the free surfaces on both sides is easy to appear instability expansion. Kotousov *et al*. (2013) found the redistribution of stress on the free surfaces and Poisson′s ratio effect can cause the additional fracture modes under shear or anti-plane loading. The main reason is that the shear or anti-plane loading generates a coupled three-dimensional anti-plane and shear singular stress state. In addition, the combined loads have also been studied. Zhang *et al*. (2015) investigated the SIFs in round bars under the combined bending and torsion loadings. Fu *et al*. (2017) used the combined *J* integral and three-dimensional finite element method to predict SIFs for inclined external surface cracks in pipes under axial tension and bending load. They found that three types of SIFs (K_I, K_{II}, K_{III}) increase with the increase of relative depth for inclined angles (15°～90°). During the process of mixed fracture assessment, all three modes of fracture take place at the crack front due to the complexity of load conditions and crack geometries (Shahani & Habibi, 2007). Therefore, a value of SIF is needed to comprehensively represent the fracture driving force in the non-planar expansion. Ling *et al*. (2017) and Choi (2009) thought the effective stress intensity factor (ESIF) can well represent the mixed mode fracture in three-dimensional state. And the ESIF is also of great guiding significance for the development of crack propagation procedures. He *et al*. (2015; 2015; 2016) developed a fatigue crack growth program (FCG-System) combined some studies such as stress intensity factor theory, crack growth angle, maximum circumferential stress criterion, crack growth rate and so on. The method was used to predict structural fatigue life in the condition of mixed mode fracture.

The discussed studies show that there are few studies on the 3D mixed mode fracture of box girder with crack damage, and most research objects are basic and simple structures, such as CT specimens, flat plates, and so on. So, it is meaningful to discuss this hot issue for box girder in combination with existing research. The objectives of this paper are to carry out the fracture assessment of box girder with transverse frame under complex loads and crack geometries. The interaction integral method (IIM) in conjunction with three-dimensional (3D) finite element model and linear elastic fracture mechanics is employed in this paper, which is utilized to investigate 3D thickness stress effect and SIFs variation along the plate thickness. In addition, the influencing factors including crack lengths, crack angles and numerous combined loads are investigated emphatically. Finally, the crack growth angle is also calculated to conduct crack propagation analysis for box girder. The findings obtained from this paper have certain scientific significance and also provide essential guiding significance for evaluating the fracture strength of box girder structure.

2. ANALYTICAL METHOD

In current, there are many methods of predicting SIFs such as *J*-integral, XFEM, interaction integral method (IIM), displacement method (DM) and so on. For mixed mode fracture (MMF) problem, it is very significant for investigating three types of SIFs (K_I, K_{II} and K_{III}). Although the *J*-integral has good accuracy for predicting SIFs and overcomes mesh dependency, but does not separate to research K_I, K_{II} and K_{III}. The DM based on displacement requires a very refine mesh around the crack tip. In addition, the XFEM has poor path independence and an unstable effect for crack front, but is available for complex structure due to simple mesh around the crack tip. Compared with these methods, IIM basically has the

advantages of *J* integral, and it can study K_{I}, K_{II} and K_{III} separately. In the 3D mode, it can also be employed to study the SIFs distribution along the crack front. There is a better advantage for studying the MMF problems.
The interaction integral is derived from the *J*-integral. In 3D cracks, the *J*-integral can be expressed as (Shih *et al*., 1986):

$$J=\lim_{\Gamma\to 0}\int_{\Gamma}\left(W\delta_{1\mathrm{i}}-\sigma_{\mathrm{ij}}u_{\mathrm{j},1}\right)n_{\mathrm{i}}d\Gamma \tag{1}$$

where W is the strain energy density, Γ is integral loop, $\delta_{1,\mathrm{i}}$ is the Kronecker delta, σ_{ij} is the stress components, i and j range from 1 to 3, n_{i} is the unit vector perpendicular to the boundary Γ. In addition, $u_{\mathrm{j},1}=\partial u_{\mathrm{j}}/\partial x_{1}$.

For linear elastic problem, the *J*-integral equals to the energy release rate, and it can be expressed as follows with the existence of all three types of fracture modes (Bowness & Lee, 1995):

$$J=\frac{K_{\mathrm{I}}^2}{E^*}+\frac{K_{\mathrm{II}}^2}{E^*}+\frac{1+\nu}{E}K_{\mathrm{III}}^2 \tag{2}$$

where ν is Poisson's ratio. E^*: $E^*=E$ (plane stress), $E^*=E/(1-\nu^2)$ (plane stress).

To separate the SIFs K_{I}, K_{II} and K_{III}, the auxiliary fields have to be introduced. By superimposing auxiliary fields and actual fields and evaluating the *J*-integral:

$$J^{\mathrm{sup}}=J+J^{\mathrm{aux}}+I \tag{3}$$

The expression I is interaction integral including the interaction between auxiliary fields and actual fields, it can be derived as (Yu *et al*., 2009):

$$I=\lim_{\Gamma\to 0}\int_{\Gamma}\left(\sigma_{\mathrm{jk}}\varepsilon_{\mathrm{jk}}^{\mathrm{aux}}\delta_{1\mathrm{i}}-\sigma_{\mathrm{ij}}^{\mathrm{aux}}u_{\mathrm{j},1}-\sigma_{\mathrm{ij}}u_{\mathrm{j},1}^{\mathrm{aux}}\right)n_{\mathrm{i}}d\Gamma \tag{4}$$

where (σ_{ij}, $\varepsilon_{\mathrm{ij}}$, u_{j}) is the actual field variable, ($\sigma_{\mathrm{ij}}^{\mathrm{aux}}$, $\varepsilon_{\mathrm{ij}}^{\mathrm{aux}}$, $u_{\mathrm{j}}^{\mathrm{aux}}$) is the auxiliary field variable.

The relationship between the interaction integral I and SIFs can be expressed as:

$$I=\frac{2}{E^*}\left(K_{\mathrm{I}}K_{\mathrm{I}}^{\mathrm{aux}}+K_{\mathrm{II}}K_{\mathrm{II}}^{\mathrm{aux}}\right)+\frac{2(1+\nu)}{E}K_{\mathrm{III}}K_{\mathrm{III}}^{\mathrm{aux}} \tag{5}$$

With the assigned values $K_{\mathrm{I}}^{\mathrm{aux}}=1$ and $K_{\mathrm{II}}^{\mathrm{aux}}=0$, $K_{\mathrm{III}}^{\mathrm{aux}}=0$, the Eq. (5) is expressed in terms of the interaction integral as follow:

$$K_{\mathrm{I}}=\frac{2}{E^*}I \tag{6}$$

Similarly, when assigning the values of $K_{\mathrm{I}}^{\mathrm{aux}}=0$, $K_{\mathrm{II}}^{\mathrm{aux}}=1$, $K_{\mathrm{III}}^{\mathrm{aux}}=0$ and $K_{\mathrm{I}}^{\mathrm{aux}}=0$, $K_{\mathrm{II}}^{\mathrm{aux}}=0$, $K_{\mathrm{III}}^{\mathrm{aux}}=1$, respectively. The K_{II} and K_{III} can be derived from Eq. (4):

$$K_{\mathrm{II}}=\frac{2}{E^*}I,\ K_{\mathrm{III}}=\frac{2(1+\nu)}{E}I \tag{7}$$

From above research, the three sets of SIFs can be expressed when each of auxiliary modes is superimposed on the actual crack field. In MMF problems, different fracture modes have a dominant effect at different stages due to complex cases. A value of SIF is needed to represent the whole crack driving force, which can derive the crack growth rate *da*/*dN*. In this study, the K_{eff} (ESIF) is used to characterize crack driving force on the integrated fracture stage. The work adopts common ESIF equation which is expressed as below (Deng *et al*., 2015; Ismail *et al*., 2012):

$$K_{\mathrm{eff}}=\left(K_{\mathrm{I}}^2+K_{\mathrm{II}}^2+\frac{K_{\mathrm{III}}^2}{1-\nu}\right)^{1/2} \tag{8}$$

3. FINITE ELEMENT ANALYSIS

3.1 GEOMETRIC MODEL AND MATERIAL PROPERTIES

A steel box girder model with transverse frame similar to the literature (Shi & Wang, 2012) is designed to carry out the fracture assessment. And the effect of initial distortion and welding residual stress is temporarily not considered. The dimension details of the model are shown in Figure 1 and Table 1. Considering that the box girder mostly bears bending and torsion loads in actual cases, this paper mainly studies the cases such as bending load, torsion load and combined loads. But the related studies also show that the side load has a certain influence on fracture analysis of box girder. Therefore, a simple side load form as an additional effect is also investigated. The materials of box girder are assumed to be homogeneous, isotropic, and linear elastic, as shown in Table 1.

Table 1. The dimension and material properties of box girder

Parameters	Value
a	100mm
b	100mm
h	100mm
t	3mm
h_0	10mm
t_0	3mm
$2c/a$	0.1~0.6
θ	0°~90°
E	206GPa
ν	0.3

3.2 FINITE ELEMENT MODEL AND BOUNDARY CONDITIONS

In this study, the 3D finite element model of box girder with transverse frame is established using the commercial code ANSYS 15.0 software. The FE model is made up of 20-node iso-parametric quadratic brick elements (Ismail *et al*., 2012), which can well investigate the SIFs distribution along the crack front. For the mesh, the singular elements with the mid-side nodes displaced to the quarter-point positions (20-node singular element) are adopted in the first layer elements to simulate the crack tip singularity. Then the other region near the crack tip adopts a fine mesh and gradually transits to a sparse mesh, as shown in Figure 2. And the reasonable mesh parameters have been selected in Table 2. In this study, the interaction integral method (IIM) is adopted to predict the SIFs in such conditions, and the obtained results are also stable and reliable (Chen *et al*., 2010).

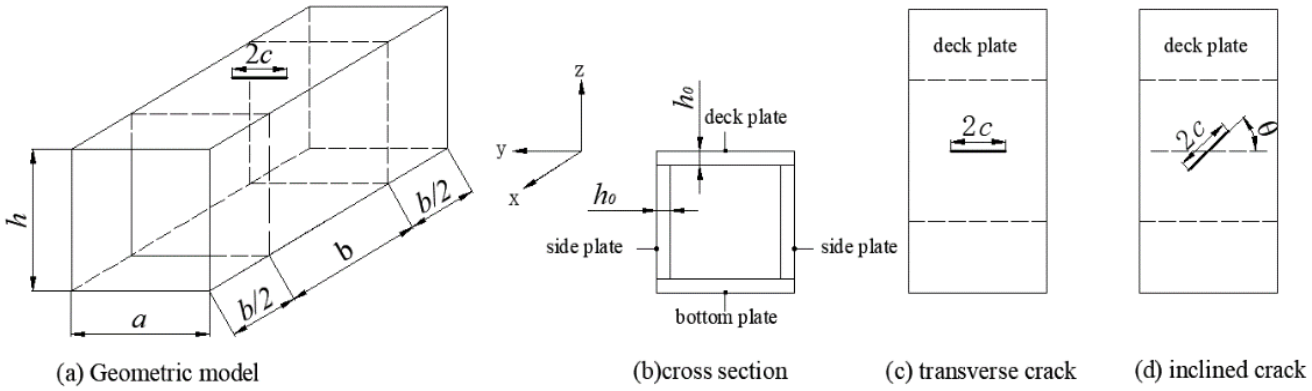

Figure 1. Geometric model

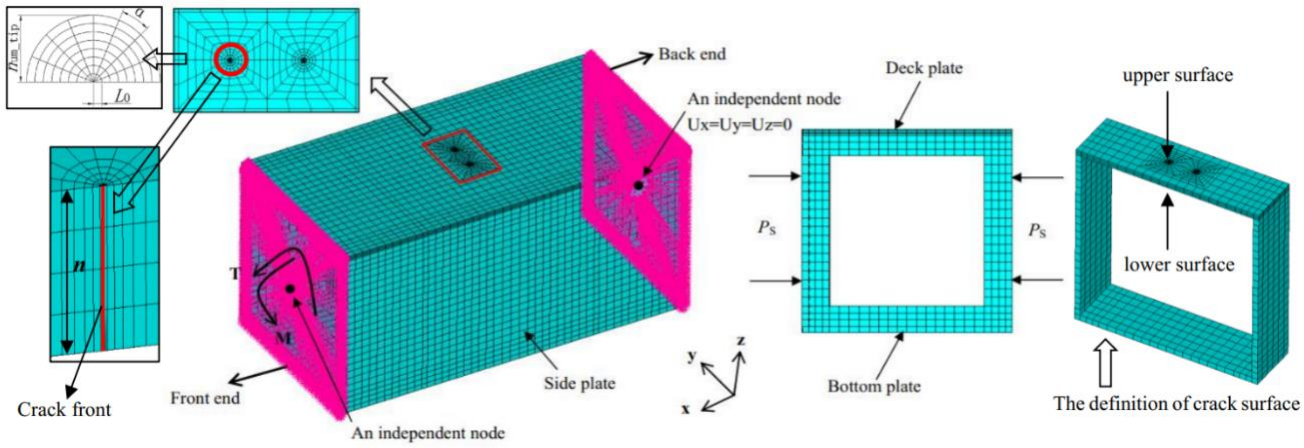

Figure 2. Finite element model and boundary condition

The details of boundary conditions are shown in Figure 2. Two independent reference nodes locate in the center of the front end and back end, respectively. The other nodes of end face and independent reference node are coupled in three displacement degrees by adopting the multi-point constraint (MPC). In the subsequent finite element analysis, a fixed constraint, $U_x = U_y = U_z = 0$, is applied on the independent reference node of back end, and the bending and the torsion loads M(My), T(Mx) are applied on the independent reference node of front end. And the uniform side load P_S is applied on two side plates.

3.3 VERIFICATION OF MESH CONVERGENCE

This work mainly studies the crack of deck plate, so the mesh of deck plate may have a certain effect on calculated results. To ensure the accuracy of the results, the related influencing coefficients (n, α, n_{um_tip} and L_0) are considered to study the mesh density in this section. According to the literature (Chen *et al*., 2010), the effects of α and n_{um_tip} on the calculated results is negligible. Therefore, this work only needs to investigate the effects of n and L_0, which may affect the SIFs distribution along the crack front and the values of SIFs. Additionally, the bending and tension loads are also used to investigate the SIFs (including K_I, K_{II} and K_{III}). As shown in Figure 3(a) and 3(b), the obtained three types of SIFs distribution near the thickness center are almost close under the different number of element layers n. And the SIFs distribution near the free face (crack location along the crack front: z / t=±0.5) is only slight difference. For the effect of singular elements, it can be seen from Figure 3(c) and 3(d) that the

SIFs distribution is also slightly different under the different size of L_0. Therefore, considering computing time and result reliability, the details of reasonable mesh parameters are determined, as listed in Table 2.

Table 2. The mesh parameters

Description	Value
Number of element layers along the thickness direction, n	4
The angle around the crack tip, α	22.5°
Number of layers around crack tip, n_{um_tip}	8
The size of singular elements, L_0	0.05mm

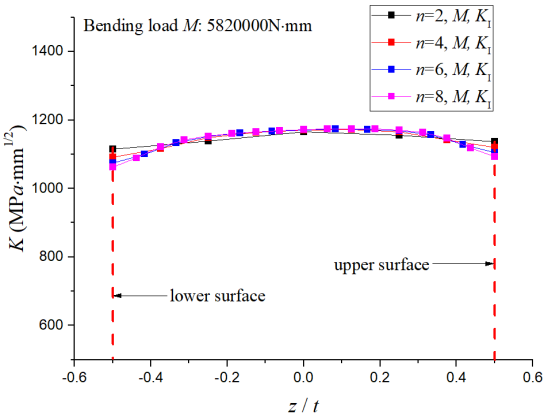

(a) The effect of n for K_I

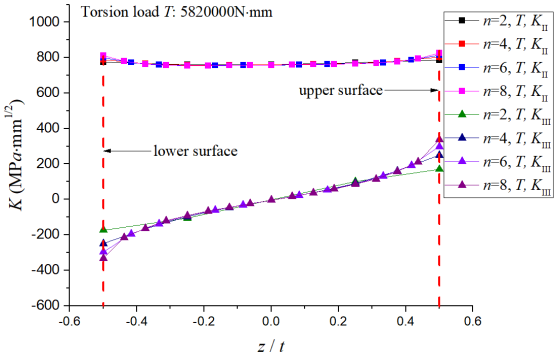

(b) The effect of n for K_{II} and K_{III}

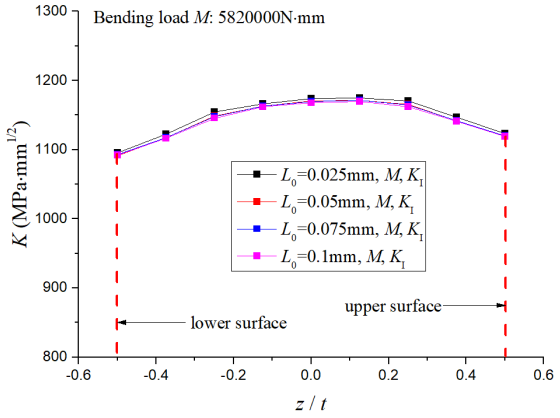

(c) The effect of L_0 for K_I

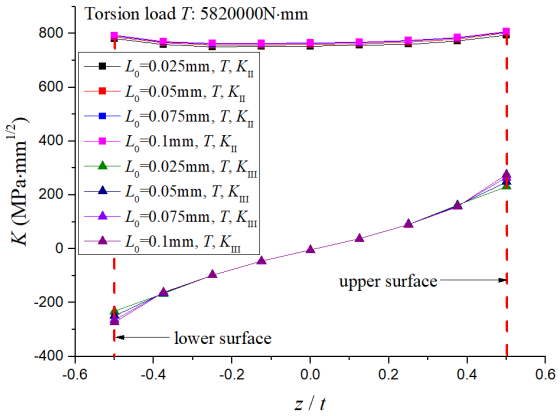

(d) The effect of L_0 for K_{II} and K_{III}

Figure 3. The effect of mesh parameters on SIFs

3.4 THICKNESS EFFECT

The analysis of SIFs in the three-dimensional state needs to consider the thickness effect (Shahani & Habibi, 2007). As shown in Figure 3, the different types of SIFs have different variations in conditions of bending load and torsion load due to the thickness effect. The variations of K_I conform to the variations law of "tunnel effect" (Zhao *et al.*, 2019), but the variations of K_{II} and K_{III} are somewhat different. The above figures show that the variations of K_{II} along the thickness direction show a " dented " trend and reach maximum value near the free surfaces. The variations of K_{III} show an "antisymmetric" trend, and also reach maximum value near the free surface. Various SIF values are obtained along the thickness direction at each crack increment, but only one SIF value is used to evaluate the fracture performance. The related literatures adopted an averaging method to express the SIF (Seo & Lee, 2002; Irfaee & Mahmound, 2019). Therefore, the equation used in this paper can be defined as below:

$$K = \sqrt{\frac{K_1^2 + K_2^2 + K_3^2 + \ldots + K_n^2}{n}} \tag{9}$$

3.5 METHOD VERIFICATION

Currently, the evaluation of SIFs for box girder is rarely touched under combined loads, and its fracture test research is not also easy to carry out due to the special characteristics of the structure. To ensure the validity of the finite element method for extracting the SIFs, the paper investigates the SIFs of the central-through cracked plate under bending load and tension load, respectively. And the mode-I fracture is considered in this analysis. As shown in Figure 4(a), the dimension details of the model are: a_1=100mm, b_1=200m, $2c_1$ / a_1=0.1~0.3 t_1=3mm. The material model parameters are: E = 206 GPa, v = 0.3. And the plate model adopts the same mesh division criteria as section 3.2. The external load (M=30000N·mm; F=15000N) is applied on the upper and lower end of the model.

As shown in Figure 4(b), the variations of K_I along the crack front show an "anti-symmetric" trend which has an obvious difference from box girder under bending load. But the variations of K_I caused by tension load are same as the case of bending load for box girder. This is probably related to the structural characteristics of box girder. The current analytical solutions are mainly proposed for the plane stress state. For the central-through cracked plate, the crack tip near the free surface (z/t_1±0.5) is closer to the plane stress state due to the lower constraint (Xu *et al.*, 2016). Therefore, this paper compares the calculation results (z/t_1=0.5) with formula solutions obtained by literature (Murakami, 1986) in Table 3. It is noted that the differences of SIFs are very small, the differences are 0.21%~0.49% in tension load condition, and the differences are 0.37%~6.7% in bending load condition. These indicate that the finite element method for extracting SIF in the paper is very reliable and reasonable. And it is not difficult to infer that this calculation method is also applicable to assess SIFs for the box girder under combined loads.

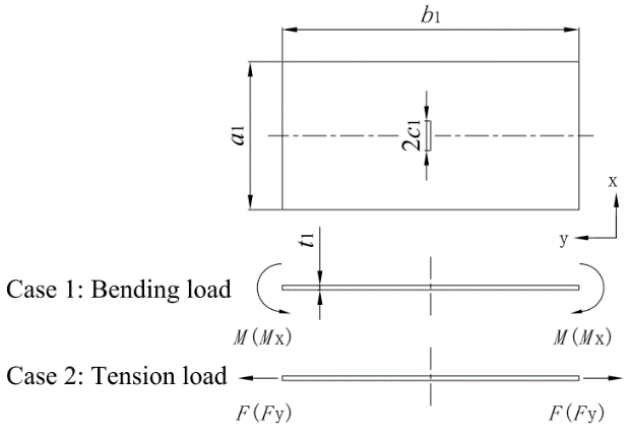

(a) Geometric model

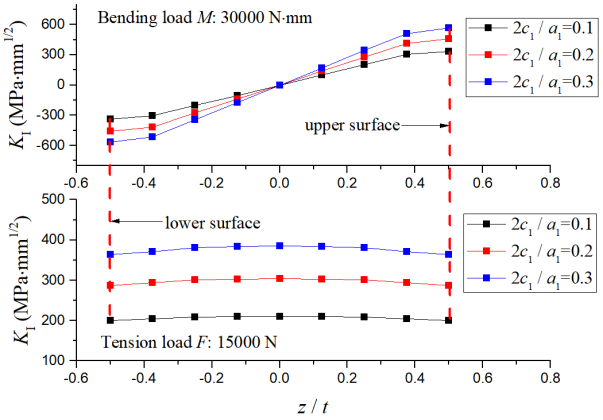

(b) The variations of K_I along the crack front

Figure 4. The plate with crack damage

Table 3. The differences of results between FEM and the literature (K_I / MPa·mm$^{1/2}$)

$2c_1$ / a_1	Case	SIFs (FEM) (z / t_1=0.5)	SIFs (Murakam, 1986)	Difference (%)
0.1	Bending	335.11	314.06	6.7
	Tension	200.28	199.3	0.49
0.2	Bending	457.51	452.09	1.2
	Tension	287.81	287.03	0.19
0.3	Bending	564.58	566.67	0.37
	Tension	363.65	362.87	0.21

4. RESULTS AND DISCUSSIONS

4.1 THE EFFECT OF BENDING LOAD

The work investigates the effect of transverse crack, inclined crack and longitudinal crack for box girder under bending load. As shown in Figure 5, it can be found that the transverse crack case (θ=0°) is most dangerous, and the fracture mode is mainly opening fracture (mode-I). The presence of inclined crack can result in mixed mode-I/II/III for box girder. When the crack angle gradually increases in the range of $0^o \le \theta \le 45^o$, K_I shows a downward trend, while K_{II} and K_{III} show an increasing trend. It may be considered that the fracture mode gradually evolves from opening fracture to sliding fracture and tearing fracture. But when the crack angle gradually increases in the range of $45^o < \theta \le 90^o$, K_I continues to decrease, while K_{II} and K_{III} also start to decrease from the highest point, which indicates that the larger crack angle can prevent crack growth. And the decreased rate of K_{eff} is gradually larger when the crack angle increases, as shown in Fig 5(b). Generally speaking, the crack of box girder is not easy to expand with the increase of inclined angle in bending load condition. Of course, when the crack type is longitudinal crack (θ=90°), the crack does not expand.

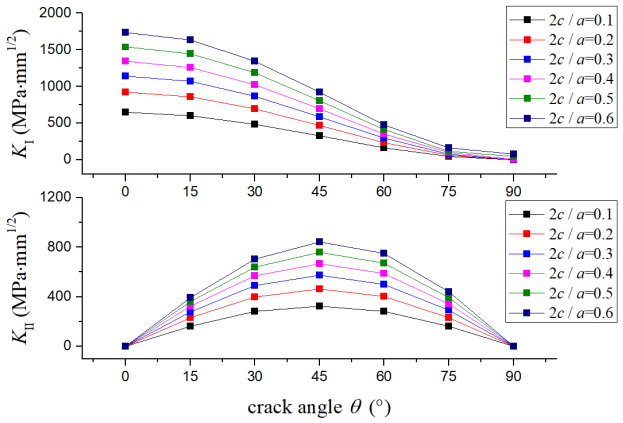

(a) The variations of K_I and K_{II}

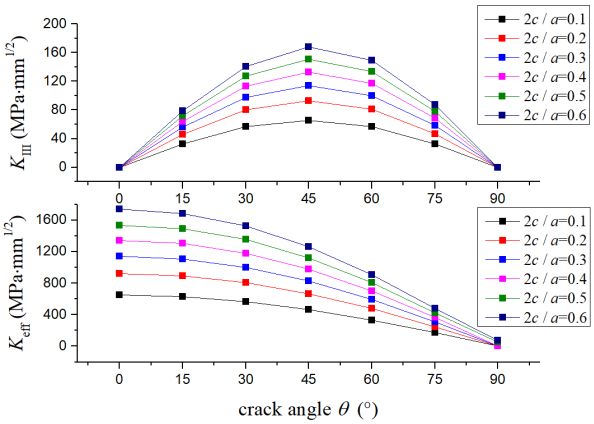

(b) The variations of K_{III} and K_{eff}

Figure 5. The variations of K under the bending load (M=5.82×10^{6}N·mm)

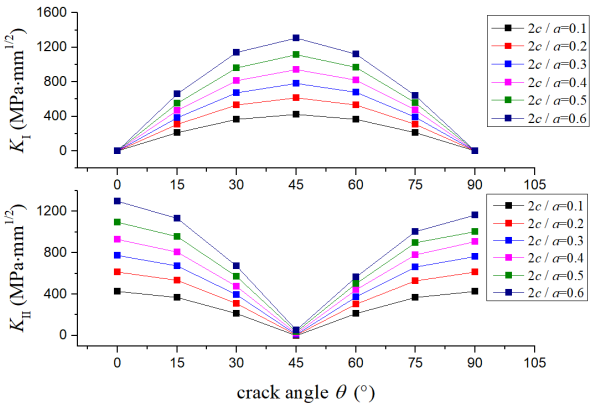

(a) The variations of K_I and K_{II}

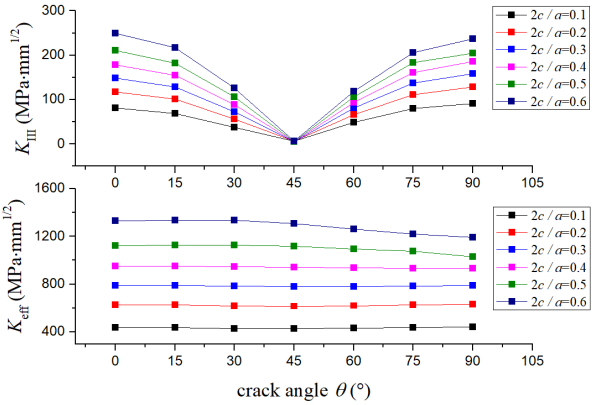

(b) The variations of K_{III} and K_{eff}

Figure 6. The variation of K under the torsion load (T=5.82×10^6 N·mm)

4.2 THE EFFECT OF TORSION LOAD

In torsion load condition, the work also investigates the effect of transverse crack, inclined crack and longitudinal crack for box girder. Under the transverse crack case (θ=0°), box girder presents mixed mode-II/III fractures. And the variation laws of K_{II} and K_{III} along the thickness direction are consistent with Figure 3. It can be considered that instability expansion easily occurs near the free surface under the effect of torsion load. The failure mode is sliding fracture (mode-II) and tearing fracture (mode-III), but sliding fracture plays a leading role.

Additionally, the effect of inclined angles is also investigated. Figure 6 shows that the variation laws of K_{II} are the same as that of K_{III}, but different from K_I. It can be seen that the fracture mode of box girder with crack angle θ=45° is mainly opening fracture. But under transverse crack and longitudinal crack cases, the fracture mode of box girder is mainly sliding fracture and tearing fracture. In general, the effect of crack angles on box girder is not obvious under torsion load according to the variation laws of K_{eff}. Only when the crack length and crack angle reach to enough large, the variations of K_{eff} show a slight downward trend.

4.3 THE EFFECT OF COMBINED LOADS

The effect of combined loads on the crack tip is different from that of a single load, which leads to complex crack propagation. Figure 7 shows the stress distribution around the crack tip under bending and torsion loads. As can be seen, the presence of bending load will make the crack faces open obviously. The stress distribution is also symmetrical under bending load, while the torsion load may change this stress distribution state. Under the case of combined loads, the presence of torsion load can make stress distribution graph emerge a certain angle which may influence the crack growth angles. When the side load is added, the stress distribution will be irregular compared to combined bending and torsion loads, and the crack front will appear to overturn. It can be considered that the stress distribution evolution behavior is an important reason for mixed mode crack propagation.

4.3.1 THE EFFECT OF CRACK TYPE

4.3.1.1 Transverse crack condition

The combined deformation can cause a certain effect on the SIFs of box girder. So, this paper studies the variations of SIFs with the different combined loads (M: T = 1: 0, 1:

1, 1: 2, 1: 3, 2: 1, 3: 1, 0: 1, Where: M: T=1: 1=2.91×10^6: 2.91×10^6) in transverse crack condition. The increased bending moment and torque will increase bending and torsion deformation of box girder to a certain extent, which can affect the variations of SIFs. Under combined loads, the box girder mainly presents mixed mode-I/II/III fractures. Table 4 and Figure 8 show that the three types of SIFs under combined loads can be obtained by adopting the linear superposition rule. According to this assumption, the SIF of every fracture mode in the case of combined loads can be expressed as:

$$\begin{cases} K_{\text{I-MT}} = K_{\text{I-M}} + K_{\text{I-T}} \\ K_{\text{II-MT}} = K_{\text{II-M}} + K_{\text{II-T}} \\ K_{\text{III-MT}} = K_{\text{III-M}} + K_{\text{III-T}} \end{cases} \tag{10}$$

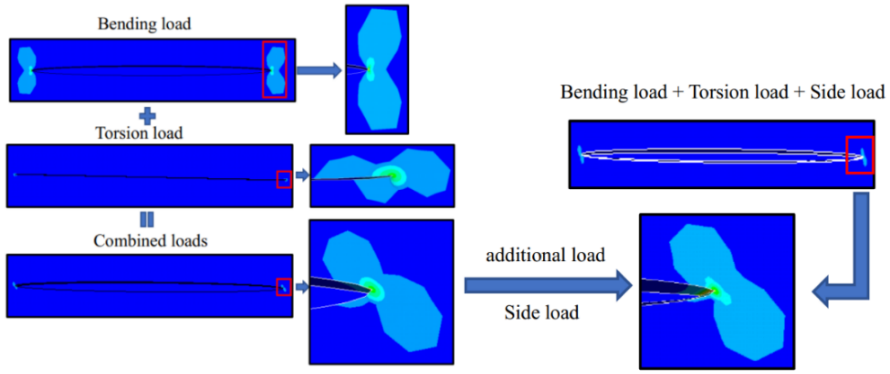

Figure 7. Crack tip evolution behaviour

Table 4. The effect of transverse cracks

K	$2c$ / a	M: T						
		1:0	1:1	1:2	1:3	2:1	3:1	0:1
K_{I}	0.1	323.9	323.9	323.9	323.9	647.8	971.7	0
	0.2	461.51	461.51	461.51	461.51	923.03	1384.55	0
	0.3	571.87	571.87	571.87	571.87	1143.74	1715.6	0
	0.4	671.61	671.61	671.61	671.61	1343.21	2014.84	0
	0.5	768.5	768.5	768.5	768.5	1536.98	2305.48	0
K_{II}	0.1	0	213.53	427.07	640.6	213.53	213.53	213.53
	0.2	0	306.68	613.35	920.03	306.68	306.68	306.68
	0.3	0	385.54	771.07	1156.61	385.54	385.54	385.54
	0.4	0	462.96	925.91	1388.88	462.96	462.96	462.96
	0.5	0	547.29	1094.58	1641.86	547.29	547.29	547.29
K_{III}	0.1	0	40.32	80.64	120.95	40.32	40.32	40.32
	0.2	0	58.76	117.52	176.28	58.76	58.76	58.76
	0.3	0	74.1	148.2	222.31	74.1	74.1	74.1
	0.4	0	89.03	178.05	267.08	89.03	89.03	89.03
	0.5	0	105.17	210.34	315.5	105.17	105.17	105.17

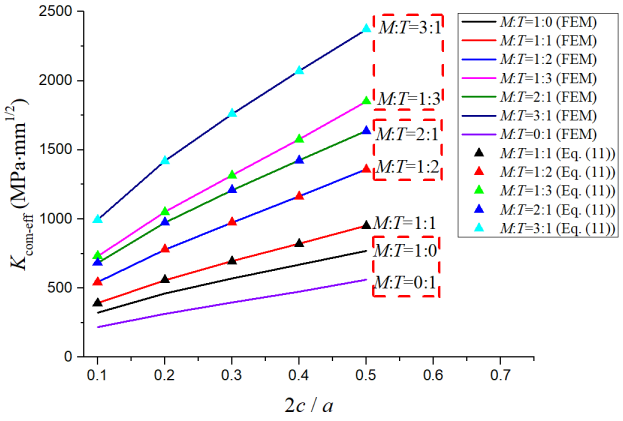

Figure 8. The variations of $K_{com\text{-}eff}$ ($2c$ / a=0.3)

Therefore, combining Eq. (8) and Eq. (10), the $K_{com\text{-}eff}$ can be expressed as:

$$K_{com\text{-}eff}=\left(\left(K_{I\text{-}MT}\right)^2+\left(K_{II\text{-}MT}\right)^2+\frac{\left(K_{III\text{-}MT}\right)^2}{1-\nu}\right)^{1/2} \qquad (11)$$

where $K_{I\text{-}M}$, $K_{II\text{-}M}$ and $K_{III\text{-}M}$ represent the three types of SIFs under bending load, respectively. And $K_{I\text{-}T}$, $K_{II\text{-}T}$ and $K_{III\text{-}T}$ represent the three types of SIFs under torsion load, respectively. $K_{I\text{-}MT}$, $K_{II\text{-}MT}$ and $K_{III\text{-}MT}$ represent the three types of SIFs under combined loads, respectively.

The $K_{com\text{-}eff}$ adopted in this study represent the whole crack driving force in the case of combined loads. Figure 8 shows that the $K_{com\text{-}eff}$ increases with the increase of crack length and load ratio. And the effect of increased bending load is greater than the increased torsion load.

4.3.1.2 Inclined crack condition

This section considers the effect of different crack angles (θ=15°~75°) on the fracture analysis of box girder in the case of combined loads. The bending and torsion loads can promote mixed mode-I/II/III fractures because of the existence of inclined cracks. As presented in Table 5 and Figure 9, the combined effect on SIFs may only be linearly superposed under the larger angle cracks ($\theta > 45^{\circ}$), which has some difference from transverse cracks. Under the small inclined crack cases, the superposition principle may be not applicable, and the results obtained from the formula are greater than that of FEM. This result may be attributed to the interaction of bending load and torsion load.

When the bending load ratios increase, K_I gradually decreases with the increase of crack angles, while K_{II} and K_{III} gradually increase first and then gradually decrease. But when the torsion load ratios increase, K_I firstly increases and then decreases with the increase of crack angles, while K_{II} and K_{III} firstly decrease and then gradually increase. It is found that three types of SIFs have complex mutual evolution with increased crack angles.

The presence of torsion load can reduce the effect of crack angles on the box girder, as shown in Figure 9. Especially when there is only torsion load, the effect of crack angles can be almost negligible. When the bending load ratios are greater than torsion load ratios (M: T>1), the effect of crack angles will be very obvious. The $K_{com\text{-}eff}$ is gradually decreasing with the increase of crack angles. On the contrary, when the torsion load ratios are great (M: T<1), the $K_{com\text{-}eff}$ only shows the small downtrend in the condition of larger crack angles. In addition, when the crack angle is approximately 47°, the values of $K_{com\text{-}eff}$ may be consistent in the case of anti-symmetric combined loads ratios (for example, anti-symmetric load ratio: M: T=1:0 and M: T=0:1; M: T=1:2 and M: T=2:1; M: T=1:3 and M: T=3:1).

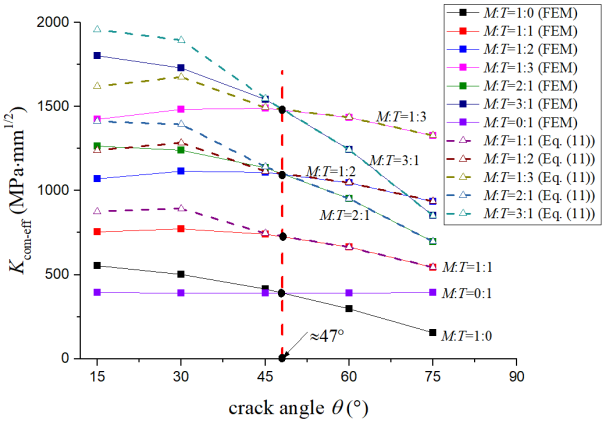

Figure 9. The variations of $K_{com\text{-}eff}$ ($2c$ / a=0.3)

4.3.2 The effect of additional side load

This analysis is to approximately simulate the effect of side load on the deck plate cracks for box girder. In this section, a simple uniform side load form (P_s= 0.5 ~ 2MPa) is considered in the cases of combined loads (M: T=1:1, 3:1, 1:3) and inclined cracks (θ=30°, 45°, 60°). Figure 10(a) indicates that the existence of side loads can largely change the distribution of K_I along the crack front, and have a certain promotion for K_{II} and K_{III}. With the increase of the side loads, the area near the crack upper surface of deck plate will be easy to expand. This response may change the fact that the crack of thickness center first to expand. In general, the effect of side load on the crack driving force has a certain promotion effect, as shown in Figure 10(b).

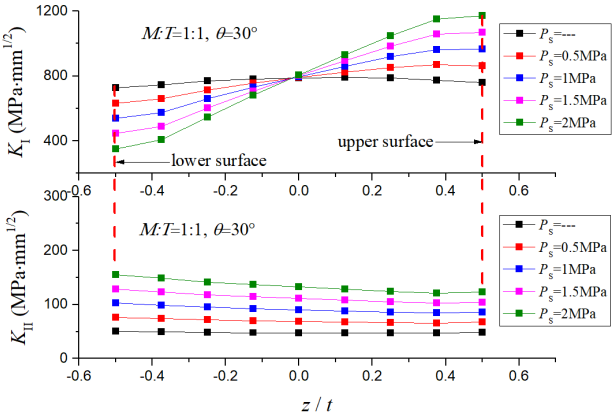

(a) The variations of K_{I} and K_{II}

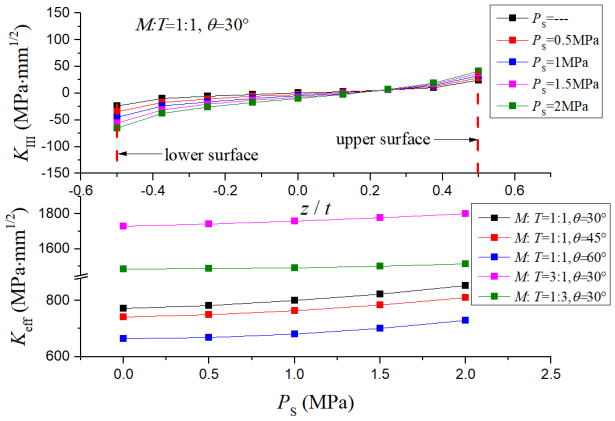

(b) The variations of K_{III} and K_{eff}

Figure 10. The variations of K with the effect of side load

Table 5. The effect of inclined cracks

K	θ (°)	M: T						
		1:0	1:1	1:2	1:3	2:1	3:1	0:1
K_{I}	15	535.29	728.5	921.72	1114.95	1263.78	1799.07	193.23
	30	433.97	769.96	1105.98	1441.99	1203.94	1637.90	336.02
	45	292.5	682.4	1072.31	1462.23	974.88	1267.37	389.93
	60	147.73	485.85	825.98	1165.11	634.57	782.29	339.14
	75	39.91	236.23	432.58	628.94	276.11	316	196.36
K_{II}	15	140.03	195.1	530.24	865.38	55.08	84.98	335.14
	30	244.85	48.31	148.26	344.81	293.15	538.0	196.55
	45	286.18	280.9	275.63	270.37	567.07	853.25	5.27
	60	250.61	438.52	626.43	814.34	689.12	939.73	187.91
	75	145.79	476.12	806.46	1136.79	621.91	767.7	330.33
K_{III}	15	27.98	36.11	100.16	164.22	8.38	20.05	64.06
	30	48.92	12.72	24.25	60.6	61.5	110.40	36.46
	45	57.18	58.96	60.8	62.7	116.12	173.29	2.69
	60	50.07	90.35	130.64	170.94	140.41	190.49	40.31
	75	29.13	97.8	166.48	235.16	126.92	156.05	68.68

4.4 THE CRACK GROWTH ANGLE ANALYSIS

Under complex loads or inclined cracks, there are mixed fracture modes including all three fracture modes along the crack front. When the SIFs reach fracture toughness, the cracks will expand non-planarly. The crack growth direction is an important fracture parameter to determine the crack growth. The maximum circumferential stress (MTS) criterion (He *et al*., 2015) and the general fracture (GF) criterion (Fu *et al*., 2017) are widely used to evaluate the mixed modes of crack growth direction. When the results of mode III (K_{III}) are very small or even negligible, the MTS criterion is applicable and effective. On the contrary, the GF criterion should be taken into account in the application.

Based on MTS criterion, the crack growth angle θ_0 can be defined as:

$$K_I \sin\theta_0 + K_{II}\left(1+\cos\theta_0\right)=0 \tag{12}$$

Then, the crack growth angle can be determined by solving the Eq. (12). Therefore, the θ_0 can be expressed as:

$$\theta_0 = 2\tan^{-1}\left(\frac{K_I}{4K_{II}} - \frac{\mathrm{sign}\left(K_{II}\right)}{4}\sqrt{\left(\frac{K_I}{K_{II}}\right)^2+8}\right) \tag{13}$$

where θ_0 is greater than zero, the crack expands in an anticlockwise direction; θ_0 is smaller than zero, the crack extends in the clockwise direction, as shown in Figure 11(a).

Based on GF criterion, the crack growth angles θ_0 can be defined as:

$$\frac{m+1}{8}\left[\begin{array}{l} K_I^2\left(\sin\frac{\theta_0}{2}+\sin\frac{3}{2}\theta_0\right)+4K_IK_{II}\cos\frac{3}{2}\theta_0 \\ -K_{II}^2\left(3\sin\frac{3}{2}\theta_0-5\sin\frac{\theta_0}{2}\right)\end{array}\right]+K_{III}^2\sin\frac{\theta_0}{2}=0 \tag{14}$$

where under plane stress, $m=3-\nu/1+\nu$; under plane strain, $m=3-4\nu$; ν is Elastic modulus.

Figure 11(b) shows the difference of the variations of crack growth angles along the crack front using MTS criterion and GF criterion, respectively. As can be seen, the difference is very slight. It can be concluded that the mode-I and mode II have the main contribution to affect crack growth for box girder fracture in complex conditions. Based on this conclusion, the MTS criterion is applicable to perform this analysis for isotropic elastic material. In addition, the variations of crack growth angles along the crack front are very gentle from the analyses without side load, and the variation curves present slight "tunnel effect". But when the side load is added, the variations of crack growth angles will be changed and reach the minimum value near the upper surface. Interestingly, it is found that the K_{eff} corresponding to this area is very large combined with Figure 10.

There is a certain correlation between the variations of the initial crack angles θ and that of crack growth angles θ_0, as presented in Figure 11 (c). The crack growth angles will increase with the increase of initial crack angles under larger bending load ratios (M: T>1). However, when torsion load ratios are larger (M: T<1), the crack growth angles will firstly decrease and then gradually increase. Additionally, it can be also found that the additional side load only has a slight effect. Combining the results of Figure 9 and Figure 11(c), it can be found that the K_{eff} is very larger when the crack growth angle is small for the same load case.

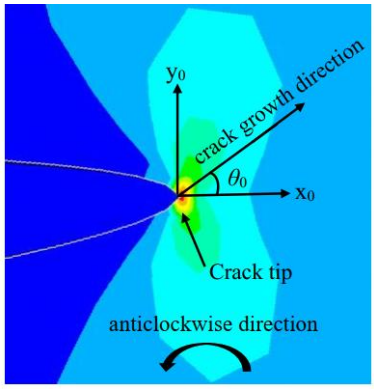

(a) Crack growth cloud

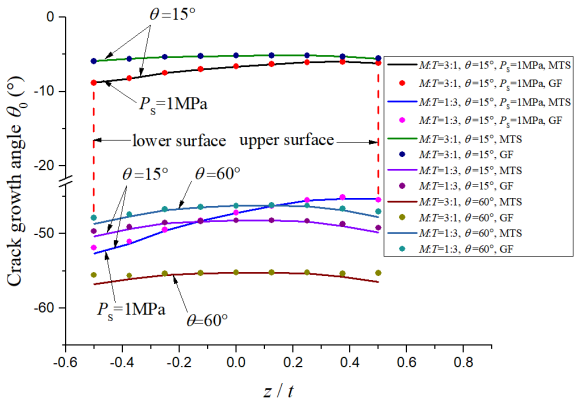

(b) Crack growth angles along the crack front

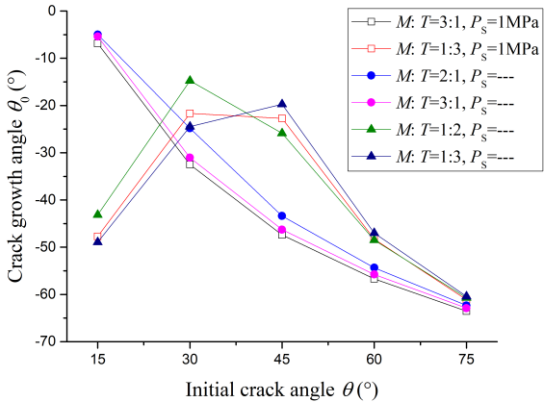

(c) The relationship between initial crack angle and crack growth angle

Figure 11. The crack growth angles under mixed mode fracture

5. CONCLUSION

This paper carries out the mixed mode fracture assessment of box girder under complex loads and crack geometries. During this research, the following conclusions can be drawn:

(1) The bending load mainly promotes opening fracture (K_I), and the torsion load mainly promotes sliding fracture (K_{II}) and tearing fracture (K_{III}). When carrying out fracture assessment for box girder, the effect of bending load should be considered emphatically.

(2) For the case of single load, with the increase of crack angles θ, the crack driving force represented by K_{eff} gradually decreases under bending load. But under torsion load, the K_{eff} has a little change with the increased crack angles θ. And only in the case of the larger crack lengths and crack angles, the torsion load may produce a small reduction for the K_{eff}.

(3) For the case of combined loads, the combined effect for three modes of SIFs may be regarded as a linear superposition in the condition of transverse cracks or larger inclined cracks. When the crack angles are small (θ<45°), the superposition principle may be not applicable, the interaction of bending moment and torque should be considered at this time. And the increased bending load ratios can lead to a great reduction of the K_{eff} with the increase of crack angles compared to the increased torsion load ratios, because the presence of torsion load may reduce the effect of inclined cracks.

(4) The side load has a great effect on the distribution of K_I (mode-I) along the crack front. With the increased side loads, the area near the crack upper surface of deck plate is more prone to occur unstable expansion.

(5) The crack growth angles θ_0 increase with the increase of the initial crack angles θ in the condition of the larger bending load ratios (such as: M: T=3:1). But in the condition of larger torsion load ratios (such as: M: T=1:3), the crack growth angles θ_0 show a trend of first decreasing and then increasing.

(6) There is a certain connection between the crack growth angles θ_0 and K_{eff}. It can be found that the K_{eff} is very larger when the crack growth angle is small for the same load case.

6. ACKNOWLEDGEMENTS

The authors are grateful for the financial support from the National Natural Science Foundation of China (Grant No. 51779198).

7. REFERENCES

1. AWANG, N., WIRZA, R., SULAIMAN, P.S., JAAFAR, A. and BENG, N.S. (2018) *Filling Sharp Features on Corner of Triangular Mesh by using Enhanced Advancing Front Mesh (EAFM) method*. International Journal of Engineering and Technology, 7, pp. 114-118. DOI: 10.14419/ijet.v7i2.14.11466.
2. AYHAN, A. O., and DEMIR, O. (2019) *A novel test system for mixed mode-I/II/III fracture tests – Part 1: Modeling and numerical analyses*. Engineering Fracture Mechanics, 218, pp. 106597. DOI: 10.1016/j.engfracmech.2019.106597.
3. ANDERSON, T. (2005) *Fracture mechanics-fundamentals and applications*. 3rd ed. CRC Press, American 2005.
4. BENVENUTI, E. (2017) *An effective XFEM with equivalent eigenstrain for stress intensity factors of homogeneous plates*. Computer Methods in Applied Mechanics and Engineering, 321, pp. 427-454. DOI: 10.1016/ j.cma.2017.04005.
5. BOWNESS, D. and LEE, M.M.K. (1995) *The development of an accurate model for the fatigue assessment of doubly curved cracks in tubular joints*. International Journal of Fracture, 73(2), pp. 129-147. DOI: 10.1007/BF00055725.
6. CUI, H.W. and YANG, P. (2018) *Ultimate strength and failure characteristics research on steel box girders under cyclic-bending moments*. Journal of Marine science and Technology, 23(4), pp. 1-11. DOI: 10.1007/s00773-017-0521-3.
7. CHEN, M., LI, M. and CHEN, W. (2018) *Analysis of crack growth based on interaction integral method*. Journal of Hunan University (Natural sciences), 45(4), pp. 74-81.
8. CHOI, Y. (2009) *A study on the effects of machining-induced residual stress on rolling contact fatigue*. International Journal of Fatigue, 31(10), pp. 1517-1523. DOI: 10.1016/ j.ijfatigue.2009.05.001.
9. CHENG, J., HUANG, Y. and LIU, G. (2010) *Analysis of Finite Element Model for Calculating Stress Intensity Factor Based on Crack-tip Singular Element*. Shipbuilding of China, 51(3), pp. 56-64.
10. DEMIR, O., AYHAN, A.O. and İRIÇ, S. (2019) *A novel test system for mixed mode-I/II/III fracture tests – Part 2: Experiments and criterion*

development. Engineering Fracture Mechanics, 220, pp. 106671. DOI: 10.1016/j.engfracmech.2019.106597.

11. DENG, S., HUA, L., HAN, X.H., WEI, W.T. and HUANG, S. (2015) *Analysis of Surface Crack Growth under Rolling Contact Fatigue in a Linear Contact*. Tribology Transactions, 58(3), pp. 432-443. DOI: 10.1080/10402004.2014.983250.
12. FU, G.Y., YANG, W. and LI, C.Q. (2017) *Stress intensity factors for mixed mode fracture induced by inclined cracks in pipes under axial tension and bending*. Theoretical and Applied Fracture Mechanics, 89, pp. 100-109. DOI: 10.1016/ j.tafmec.2017.02.001.
13. HOU, S., ZHU, Y., QIU, J. and SUN, X. (2018) *Accuracy analysis on the empirical equation of finite thickness semi-elliptical surface crack based on interaction integral method*. Journal of Mechanical Strength, 40(6), pp. 1479-1484. DOI: 10.16579/j.issn.1001.9669.2018.06.034.
14. HUANG, X.L., LIU, Y.H., HUANG, X.B. and DAI, Y.W. (2017) *Crack arrest behavior of central-cracked stiffened plates under uniform tension*. International Journal of Mechanical Sciences, 133, pp. 704-719. DOI: 10.1016//j.ijmecsci. 2017.09.040.
15. HE, W., LIU, J. and XIE, D. (2015) *Analysis of Fatigue Crack Growth in Longitudinals of Ship Hull and Fatigue Life*. Shipbuilding of China, 56(2), pp.1-10.
16. HE, W., LIU, J. and XIE, D. (2016) *Life assessment of fatigue crack growth of typical details in hull longitudinals*. Journal of Ship Mechanics, 20(11), pp. 1475-1484.
17. HE, W., LIU, J. and XIE, D. (2015) *Probabilistic life assessment on fatigue crack growth in mixed-mode by coupling of Kriging model and finite element analysis*. Engineering Fracture Mechanics, 139, pp. 56-77. DOI: 10.1016/j.engfracmech.2015.03.040.
18. IRFAEE, M. and MAHMOUD, H. (2019) *Mixed-Mode Fatigue and Fracture Assessment of a Steel Twin Box-Girder Bridge*. Journal of Bridge Engineering, 24(7), pp. 1-16. DOI: 10.1061/(ASCE)BE. 1943-5592.0001424.
19. ISMAIL, A.E., ARIFFIN, A.K., ABDULLAH, S.B. and GHAZALI, M.J.B. (2012) *Stress intensity factors for surface cracks in round bar under single and combined loadings*. Meccanica, 47(5), pp. 1141-1156. DOI: 10.1007/ s11012-011-9500-7.
20. KOTOUSOV, A., LAZZARIN, P., BERTO, F. and POOK, L.P. (2013) *Three-dimensional stress states at crack tip induced by shear and anti-plane loading*. Engineering Fracture Mechanic, 108, pp. 65-74. DOI: 10.1016/j.engfracmech.2013.04.010.
21. LI, Q.F. (2007) *Fracture Mechanics and Engineering Applications*, Harbin, 2007.
22. LI, Q.F., QI, G., ZHU, L. and HE, S. (2011) 3D finite element computational fracture analysis of an MCTS specimen. Journal of Harbin Engineering University, 32(9), pp. 1157-1162. DOI: 10.3969/ j.issn.1006-7043. 2011.09.011.
23. LING, J.X., SUN, W., YANG, X.J., LIAN, G.F. and JIANG, J.B. (2017) *Analysis of stress intensity factors for a TBM cutter head crack in complex stress states*. Journal of Harbin Engineering University, 38(4), pp. 633-639. DOI: 10.11990/jheu.201603104.
24. LI, L., DENG, Y.S., MENG, L.Q., PENG, C.P. and LIU, J.C. (2020) *Stress intensity factor of complex cracks in thin-walled box girder under bending*. Journal of Mechanical Strength, 43(1), pp. 211-216.
25. MURAKAMI, Y. (1986) *Stress Intensity Factor Handbook*. New York: Pergamon Press. DOI: 10.1115/1.2900983.
26. PANG, J.H.L., KIN, S.T. and HSIN, J.H. (2016) *3D stress intensity factors for weld toe semi-elliptical surface cracks using XFEM*. Marine Structures, 48, pp. 1-14. DOI: 10.1016/ j.marstruc.2016. 04.001.
27. PENG, Y. and YANG, P. (2020) *Analysis of dynamic stress intensity factors for cracked stiffened plates based on extended FE method*. International Journal of Maritime Engineering, 162(A1), pp. A35-A45. DOI No: 10.3940/ rina.ijme.2020.a1.547.
28. SHI, G.J. and WANG, D.Y. (2012) *Residual ultimate strength of cracked box girders under torsional loading*. Ocean Engineering, 43, pp. 102-112. DOI: 10.1016/j.oceaneng.2011.12.028.
29. SEIFI, R. and OMIDVAR, N. (2013) *Fatigue crack growth under mixed mode I + III loading*. Marine Structures, 34, pp. 1-15. DOI: 10.1016/ j.marstruc.2013.07.001.
30. SHAHANI, A.R. and HABIBI, S.E. (2007) *Stress intensity factors in a hollow cylinder containing a circumferential semi-elliptical crack subjected to combined loading*. International Journal of Fatigue, 29(1), pp. 128–140. DOI: 10.1016/ j.ijfatigue.2006.01.017.
31. SHIH, C.F., MORAN, B. and NAKAMURA, T. (1986) *Energy release rate along a three-dimensional crack front in a thermally stressed body*. International Journal of Fracture, 30(2), pp. 79-102. DOI: 10.1007/BF00034019.
32. SEO, D.C. and LEE, J.J. (2002) *Fatigue crack growth behavior of cracked aluminum plate repaired with composite patch*. Composite Structures, 57(1/4), pp. 323-330. DOI: 10.1016/S0263-8223(02)00095-8.
33. XUAN, Z.C., KHOO, B.C. and LI, Z.R. (2006) *Computing bounds to mixed-mode stress intensity factors in elasticity*. Archive of Applied

Mechanics, 75(4-5), pp. 193-209. DOI: 10.1007/s00419-005-0388-3.

34. XU, L., ZHANG, N., ZHOU, S., WANG, L., MA, C. and LIU, P. (2016). *Finite element analysis of through thickness effects on 300m steel stress intensity factor*. Journal of Mechanical Strength, 38(1), pp. 167-172. DOI: 10.16579/j.issn.1001.9669.2016.01.031.
35. XIONG, G., WU, X., LUO, Y.H. and WEN, M.L. (2016) *Fracture analysis and finite element simulation of crane box girder structure containing defects*. Machinery Design & Manufacture, 4, pp. 207-210.
36. YU, H.J., WU, L.Z., GUO, L.C., DU, S.Y. and HE, Q.L. (2009) *Investigation of mixed-mode stress intensity factors for nonhomogeneous materials using an interaction integral method*. International Journal of Solids & Structures, 46(20), pp. 3710-3724. DOI: 10.1016/ j.ijsolstr. 2009.06.019.
37. ZHANG, Y., HUANG, X.P. and YAN, X.S. (2015) *Stress intensity factors of surface cracks in round bars under combined bending and torsion loads*. Ship Science and Technology, 37(11), pp. 14-20.
38. ZHAO, H., LV, Y. and DOU, P.P. (2019) *Research on thickness effect of three-dimensional crack propagation path*. Journal of Ordnance Equipment Engineering, 40(8), pp. 219-225.

